



Scholars Research Library

Archives of Applied Science Research, 2011, 3 (4):280-295
(<http://scholarsresearchlibrary.com/archive.html>)



Growth, structural, optical, mechanical and electrical properties of amino acid single crystal of γ - glycine

R. Surekha^{a*}, R. Gunaseelan^b, S. Selvakumar^c P. Sagayaraj^b and K. Ambujam^d

^{a*}Department of Physics, Prathyusha Institute of Technology & Management, Tiruvallore Dt, India

^bDepartment of Physics, Loyola College, Chennai, India

^cDepartment of Physics, L.N. Govt. Arts College, Ponneri, India

^dDepartment of Physics, Queen Mary's College, Chennai, India

ABSTRACT

An organic nonlinear optical single crystal of gamma glycine (GGLY) has been grown by slow evaporation of the saturated solution at room temperature. Single crystal of gamma glycine (GGLY), an organic nonlinear optical (NLO) material, has been grown by slow solvent evaporation technique. Good optical quality single crystals with dimension up to $31 \times 30 \times 6$ mm³ are obtained. The crystals are characterized by optical absorption spectrum, FTIR and X-ray diffraction studies. The dielectric response of the sample is studied as a function of frequency and temperature. The mechanical, photoconductivity and ac/dc behavior of the grown crystals are also investigated.

Key words: NLO materials; Crystal growth; Dielectric measurement; Conductivity; Mechanical properties.

INTRODUCTION

The Quest and demand for NLO materials is always high due to its practical applications in optical modulation, switching and other signal processing devices. Manufacturing of NLO devices is limited by inorganic oxide crystals like potassium niobate that have shortcomings due to difficulty in synthesis, lack of optical quality and slow electro-optic response times. The research on organic and semi-organic crystals was started in 1980s. Organic materials offer good optical response time, non-resonant susceptibility, second harmonic generation and high phase-conjugate reflectivity [1].

Amino acids and their complexes belong to a family of organic materials that have been considered for photonic applications [2]. Amino acids are fascinating materials for NLO applications. The significance of amino acids in NLO applications is due to the fact that all the amino acids have chiral symmetry and crystallize in noncentro-symmetric space groups [3]. Out of 20 amino acids glycine is the simplest of all. Glycine family crystals have been subjected to extensive research by several researches for their efficient NLO properties [3-6]. Glycine is the only protein forming amino acid without a centre of chirality and is optically inactive too. It exists as dipolar ions in which the carboxyl group is present as a carboxylate ion and the amino group as an ammonium ion. Its high melting point is due to its dipolar nature. Under different conditions, glycine crystallizes in 3 kinds of polymorphs with different thermal stabilities [7]. Also α , β and γ glycine exhibit different characteristics. Both α and β forms are crystalline in centrosymmetric space group $P2_1/c$ that is not feasible for optical second harmonic generation [8-9]. But γ glycine crystallizes in non centrosymmetric space group $P3_1$ enabling itself ideal for piezo electric and NLO applications. Due to the presence of chromophores namely amino groups, carboxyl group, γ glycine finds itself absolutely transparent in the U-V visible region [7].

It has been reported by many researchers that single crystals of GGLY can be grown from aqueous solutions of glycine which can be acidic as well as basic [6-12]. The growth of single crystals of GGLY from aqueous solution incorporated with sodium chloride (NaCl) has been reported recently by Srinivasan and Arumugam employing slow solvent evaporation technique [13]. Ambujam et al [14] and Ramachandran et al [15] have successfully crystallized GGLY via gel technique. A scaled quantum mechanical force field calculations on the Gamma Crystal polymorph have confirmed the effect of hydrogen bond stretching in vibrational analysis [15]. Gamma Glycine is actually grown by many conventional methods like slow cooling, slow evaporation as well as gel method. Though there are numerous reports on this title compound wherein mixed solvents like water with sodium acetate, ammonium sulphate, lithium bromide [12-14] are used, still the indispensable characteristics of gamma glycine urges the researches to implant deeper studies on its properties. Bharaniraj et al have been reported the growth of gamma glycine from the aqueous solutions of alpha glycine and sodium acetate with deionised water. The present article also addresses the growth of GGLY crystals in the presence of hydrofluoric acid (HF) which is a weak hydrohalic acid investigates the possible modifications in the growth conditions as well as the physico-chemical properties of the samples. The crystals of GGLY grown with HF are characterized by single crystal and powder XRD, NLO test, optical, microhardness, dielectric and photoconductivity studies.

MATERIALS AND METHODS

2. Experimental procedure

2.1 Synthesis

Single crystals of Gamma Glycine (GG) crystals were grown by slow evaporation method at ambient room temperature. The commercially available analar grade Glycine (99.5%) and Hydrofluoric acid (40 % Merck) are taken in the ratio of 2:1 for the experiment. The solvent used for dissolving the above constituents is double distilled Millipore water and analar grade acetone mixed in the ratio of 1:1.

2.2 Solubility determination

The solubility of GGLY was determined by dissolving the synthesized product in Millipore water in an airtight container kept in a constant temperature bath, the content was continuously stirred for 2-3 hours. After attaining the saturation, the equilibrium concentration of the solute was estimated gravimetrically. The same process was repeated for different temperatures (30, 35, 40, 45, 50 and 55 °C). The variation of solubility with temperature Fig. 1 indicates that γ -glycine with HF have high positive solubility-temperature co-efficient values.

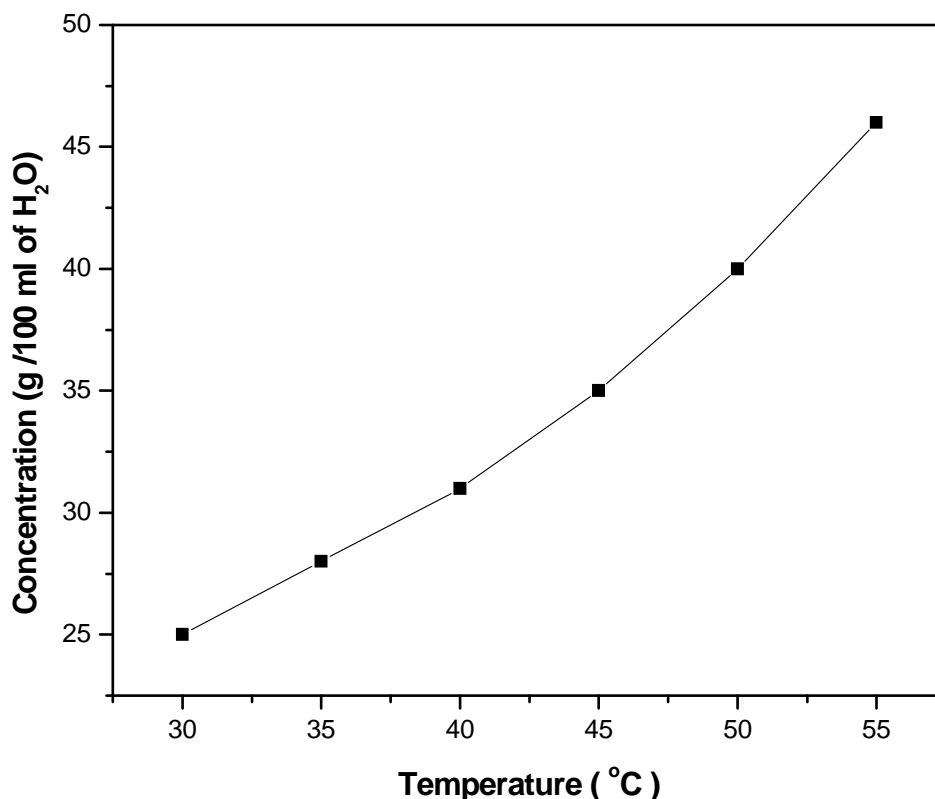


Fig. 1 Solubility curve of GGLY

2.3 Crystal Growth

The synthesized salt of GGLY is purified by repeated crystallization and saturated solution is prepared in accordance with the solubility. Since Hydrofluoric acid (HF) has the ability to react with silica compounds, only teflon experimental beakers are used. The optimized pH is measured to be 3.5 respectively. Saturated aqueous solution of GGLY is taken in a crystallizing vessel with perforated covers and placed in a constant temperature bath. Seed crystals are harvested within few days. A suitable seed crystal is selected from the harvested crystals. A saturated solution is prepared and the seed crystal is hung inside the solution that is optimally closed for controlled evaporation. By slow evaporation of the solvent, GGLY single crystal of size 31 x 30 x 6 mm³ is grown in a period of 25-30 days. The resulting crystals are of colorless needles. The grown crystals are stable, do not decompose in air and non-hygroscopic in nature. Fig. 2 shows the photograph of the as grown crystals of GGLY. An important observation during the growth of

GGLY is the absence of any kind of microbial contamination during the growth period even when the solution was kept for nearly 2-3 months. This could be attributed to the high concentration of hydrofluoric acid used in the solution.

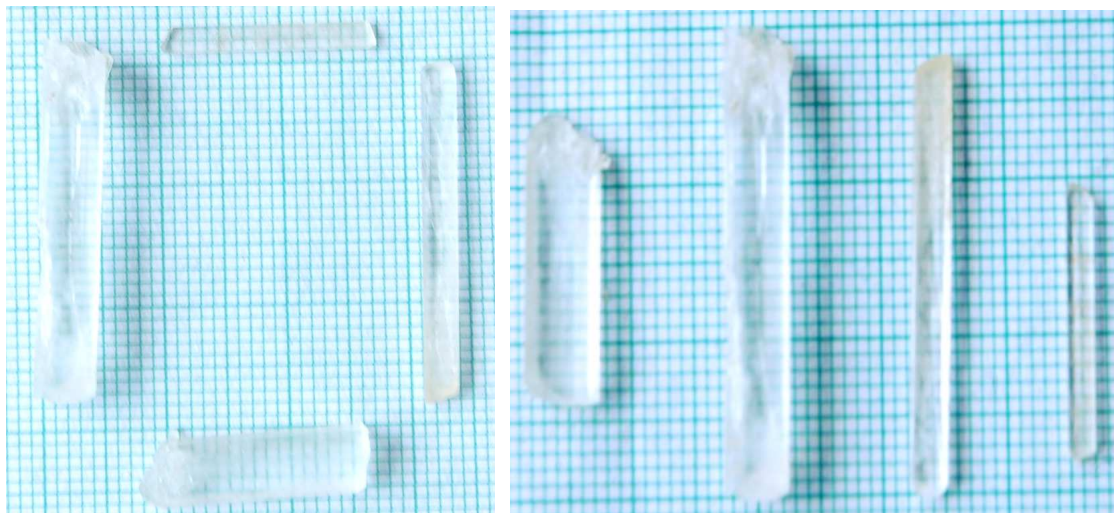


Fig. 2 Photograph of as grown from HF single crystal of GGLY

2.4 Characterization

The grown crystal of GGLY was confirmed by single crystal X-ray diffraction analysis. Single crystal XRD data was collected by ENRAF NONIUS CAD4-F single crystal X-ray diffractometer with MoK_α ($\lambda=0.71073 \text{ \AA}$) radiation. The grown crystals of GGLY were confirmed by powder XRD analysis. In this system, a fine focus ($0.4 \times 8 \text{ mm}$; 2 kW Mo) X-ray source energized by a well-stabilized Philips X-ray generator (PW 1743) was employed. The FT-IR spectrum was recorded using BRUKER IFS-66V FT-IR spectrometer with KBr pellet technique for the range $4000 - 400 \text{ cm}^{-1}$. The linear optical properties of the crystals were examined between 200 and 2000 nm using the VARIAN CARY 5E UV-Vis-NIR spectrophotometer. The powder SHG measurement was done using Nd:YAG laser fundamental ($\lambda = 1064 \text{ nm}$) radiation. In the present work, HVM SHIMADZU microhardness tester, fitted with diamond Vickers pyramidal indenter was used. The static indentations were made at room temperature with a constant indentation time of 15 seconds for all indentations. Indentations were made by varying the loads from 10 to 50 g ; above this load micro cracks are observed. Good quality single crystals of GGLY (grown with HF) were selected for dielectric measurements. Silver paint was applied on opposite faces of $(1\ 1\ 2)$ and $(1\ 1\ 0)$ planes of the crystal grown with HF, respectively, to make a capacitor with the crystal medium. The dielectric constant (ϵ_r) and dielectric loss ($\tan \delta$) of the samples were determined by measuring the capacitance and dissipation factor as a function of frequency (100 Hz - 5 MHz) and temperature ($T = 308\text{--}368 \text{ K}$), using a HIOKI-3532 LCR HITESTER. Care was taken not to perform the experiment above the phase transition temperature (443 K) of the sample.

RESULTS AND DISCUSSION

3.1 Structural studies

3.1.1 Single crystal XRD analysis

The structure of GGLY was solved by the direct method and refined by the full matrix least-squares fit technique employing the SHELXL program. It is observed that GGLY crystal crystallizes in the Hexagonal system with space group $P3_2$. The lattice parameters are $a = 7.035 \text{ \AA}$, $b = 7.037 \text{ \AA}$, $c = 5.476 \text{ \AA}$ and volume $V = 234.82 \text{ \AA}^3$. The single crystal XRD data is obtained in the present work coincides with the previously reported work [2].

3.1.2 Powder XRD analysis

The Powder XRD pattern of the grown crystals was recorded using D8 Advanced Bruker Powder X-ray Diffractometer. The positions of the peaks are found to be matching with the literature [7]. Fig. 3 depicts the powder XRD pattern of the γ glycine crystals.

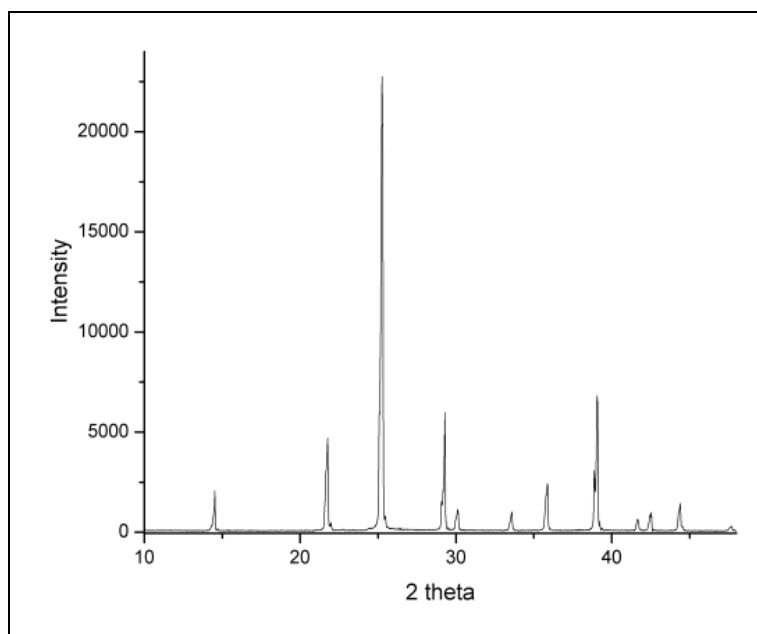


Fig. 3 Powder XRD data of GGLY grown from HF

3.1.3 FT-IR Spectroscopic Studies

This analysis was accomplished to identify the functional groups present in the grown crystal. For this, an Alpha-T/Bruker Spectrometer was used in the frequency range $400 - 4000 \text{ cm}^{-1}$. The sample used was in pellet form in KBr phase. The FT-IR spectrum is depicted in the Fig .4 which was found to be matching with the literature [7].

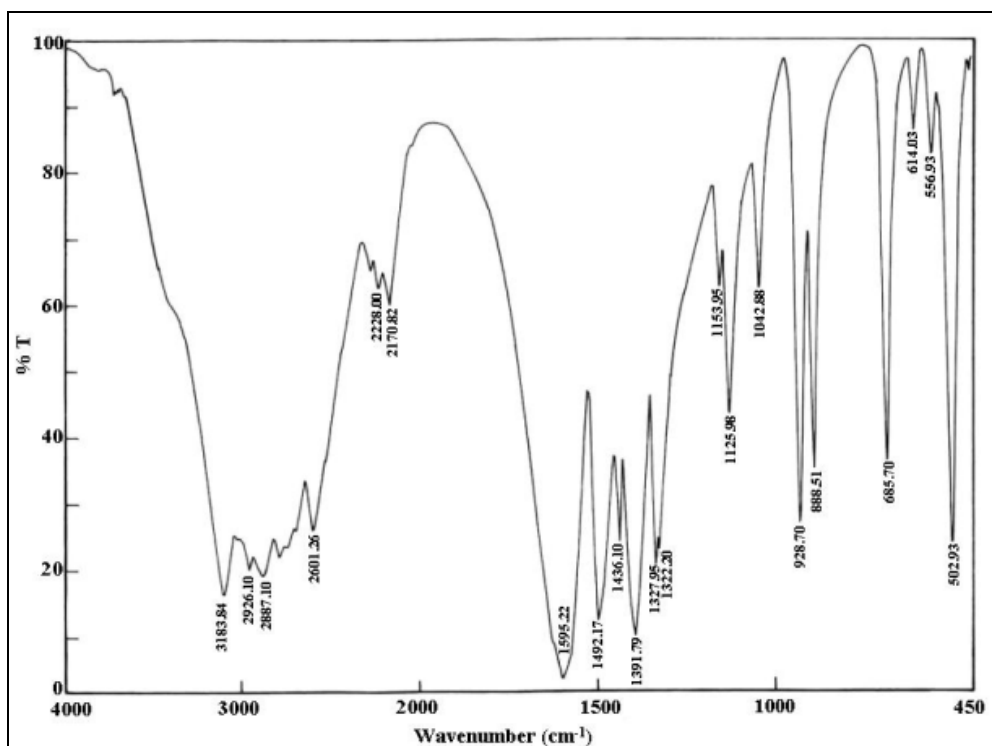


Fig. 4 FT-IR Spectrum for GGLY grown from HF

Table 1 FT-IR spectral assignments for GGLY

Wavenumber (cm ⁻¹)	Assignments
2926.10	N-H asymmetric stretch
2170.82	Combination and overtone bands
1595.22	-COO ⁻ asymmetric stretch
1492.17	NH ₃ ⁺ symmetric bending
1436.10	-CH ₂ bend
1391.79	-COO ⁻ symmetric stretch
1327.95	-CH ₂ wag
1322.20	-CH ₂ twist
1153.95	NH ₃ ⁺ rock
1125.98	NH ₃ ⁺ rock
1042.88	-CCN asymmetric stretching
928.70	-CH ₂ rock
888.51	-CCN symmetric stretching
685.70	-COO ⁻ bend
614.03	-COO ⁻ wag
556.93	NH ₃ ⁺ torsion
502.93	-COO ⁻ rock

3.2 Optical properties

3.2.1 UV-VIS-NIR spectroscopy study

Nonlinear optical single crystals are mainly used in optical applications. The optical absorption range and the cut-off wavelength are the most important optical parameters for laser frequency applications. Fig. 5 represents the optical absorption spectrum of GGLY. The UV cut-off wavelength of the sample is found to be at 350 nm and the absorption is very less in the entire visible region and part of IR region. The optical band gap is obtained by plotting the graph between $h\nu$ and $(\alpha h\nu)^2$ (Fig. 6). From the graph, the optical energy gap of GGLY is determined as 3.7 eV.

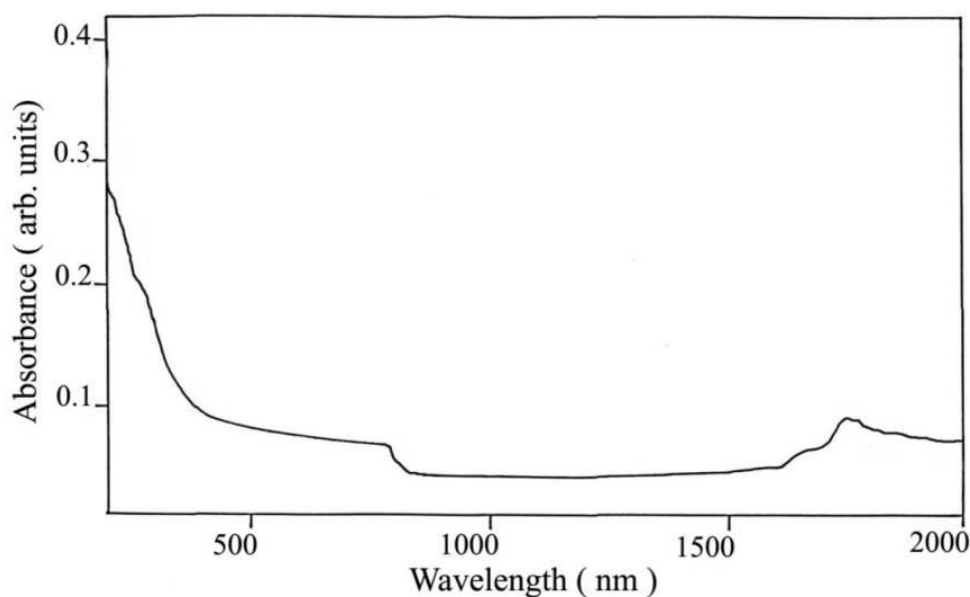


Fig. 5 Optical absorption spectrum of GGLY crystal

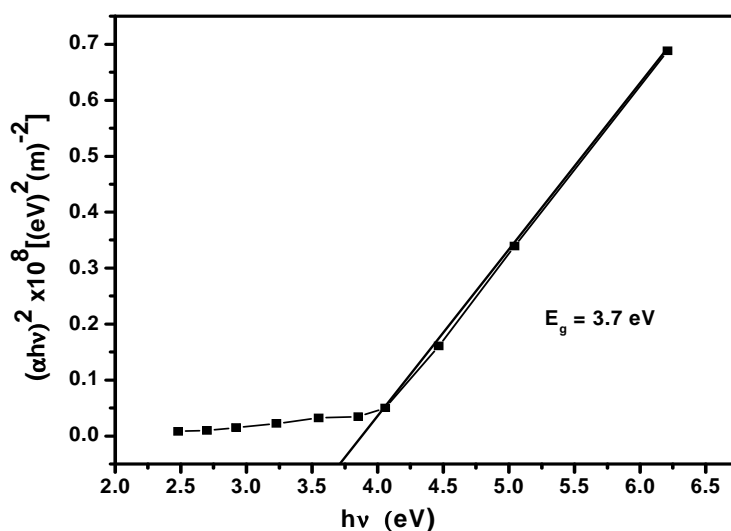


Fig. 6 Tauc's plot of GGLY

3.2.2 NLO studies

Kurtz and Perry powder SHG test was carried out on grown GGLY single crystals to study the NLO properties. The second harmonic generation (SHG) test on the GGLY crystal is performed by Kurtz powder SHG method [16]. The fundamental beam of Nd: YAG laser with 1064 nm wavelength, pulse duration of 8 ns and 10 Hz repetition rate is focused onto the powdered sample of GGLY and KDP. When the input pulse of 3.2 mJ is passed through the sample and KDP, output signals of 55 and 112 mV are obtained from GGLY and KDP respectively. It is observed that the NLO efficiency of GGLY is two times more that of KDP crystal.

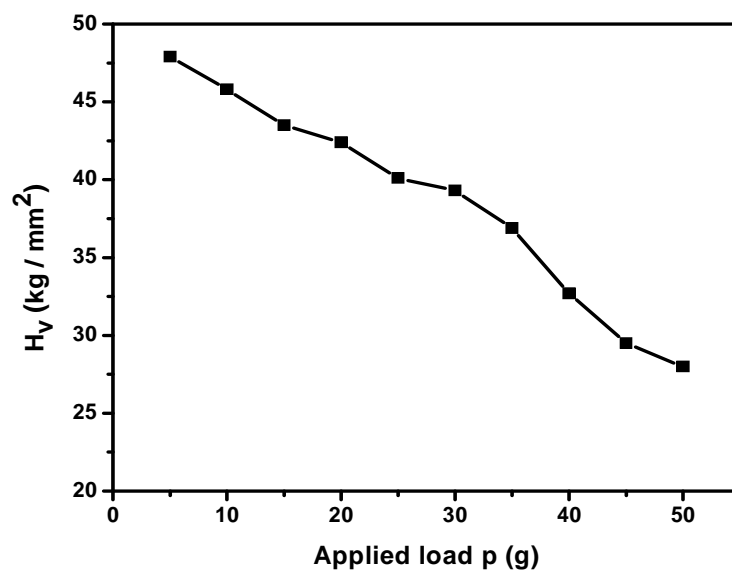


Fig. 7 Variation of Vickers Hardness Number with the applied load for GGLY

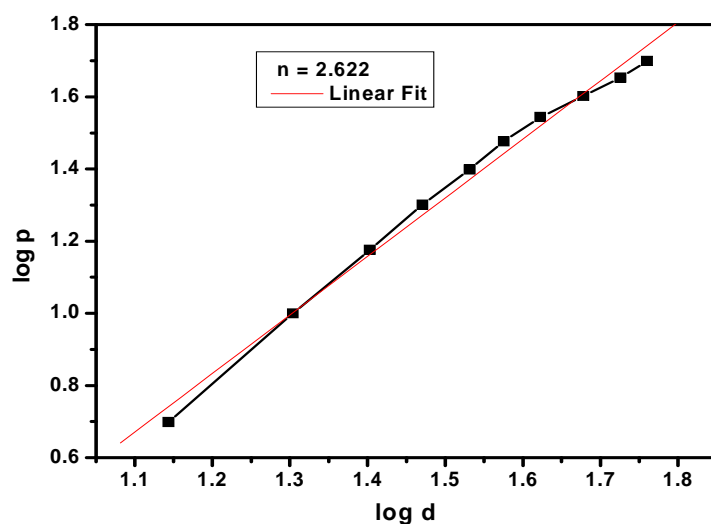


Fig. 8 Plot of $\log d$ versus $\log p$ for GGLY

3.3 Microhardness studies

A plot between the hardness number and the applied load is depicted in Fig. 7. It is evident from the figure that the Vickers Hardness number (H_v) decreases with applied load (p). This indicates that the crystal exhibits normal indentation size effect behavior (ISE). A plot drawn between $\log p$ and $\log d$ is shown in Fig. 8. From the graph the work hardening coefficient (n) is calculated using linear fit method and is found to be 2.622. Hence it supports normal ISE behavior of GGLY single crystal [17].

3.4 Electrical properties

3.4.1 Dielectric studies

Fig. 9 shows the plot of dielectric constant (ϵ_r) versus \log frequency for 308, 328 and 348 K. It is seen that the value of dielectric constant is high in the lower frequency region for all the temperatures and then it decreases with increase in frequency up to 10 kHz. The high value of dielectric constant at low frequency is attributed to space charge polarization due to charged lattice defects [18]. Beyond 10 kHz, it is almost constant and is saturated at higher frequencies. A graph is drawn between dielectric loss and \log frequency for various temperatures (308, 328 and 348 K) and is shown in Fig. 10. The low value of dielectric loss at high frequency suggests that the GGLY crystals possess good optical quality. This parameter is of vital importance for nonlinear optical materials in their applications [19]. The temperature dependence of dielectric constant and dielectric loss for various frequencies are shown in Fig. 11 and 12.

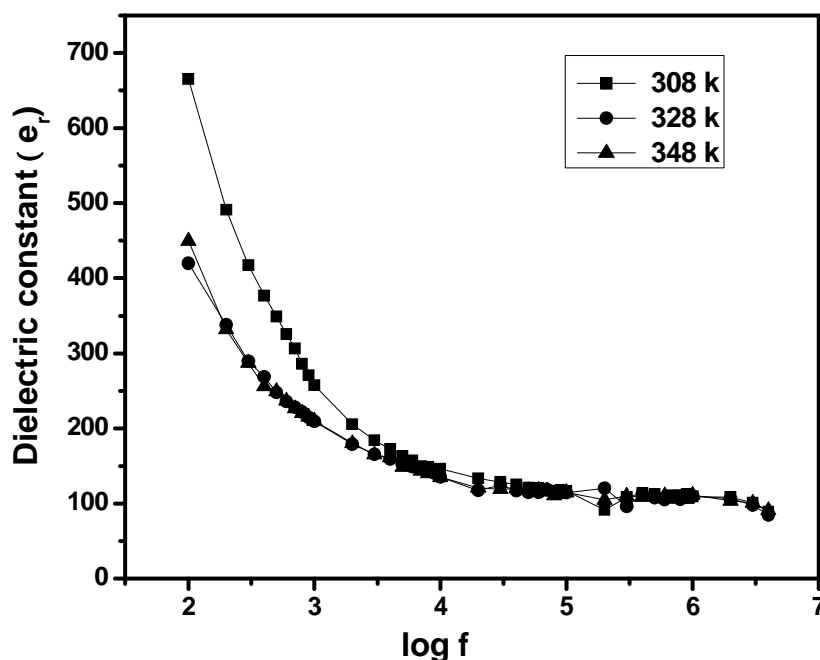


Fig. 9 Variation of dielectric constant with \log frequency for GGLY

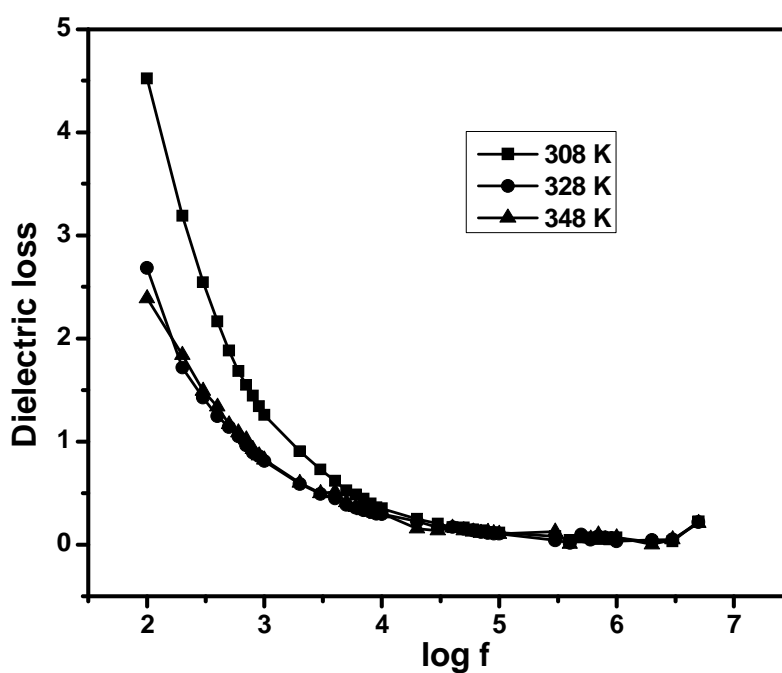


Fig. 10 Variation of dielectric loss with log frequency for GGLY

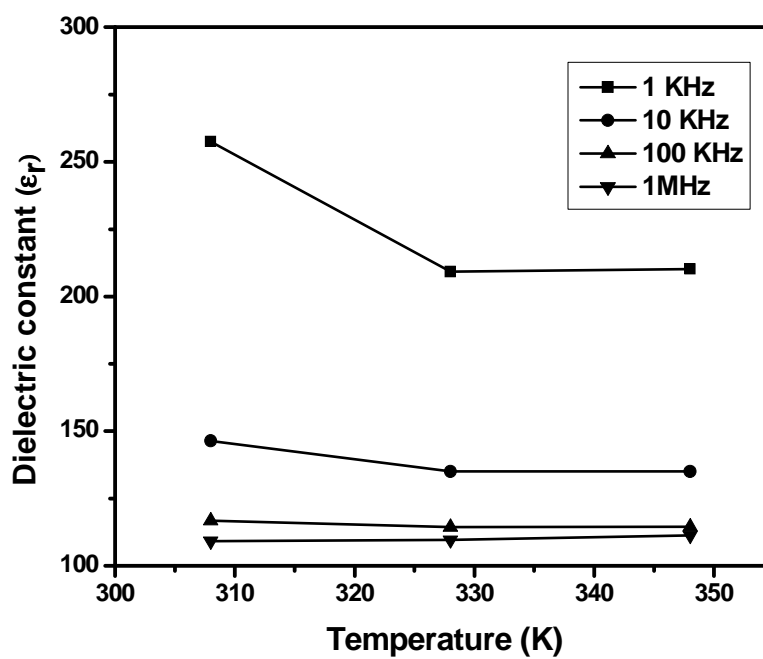


Fig. 11 Temperature dependence of dielectric constant for GGLY

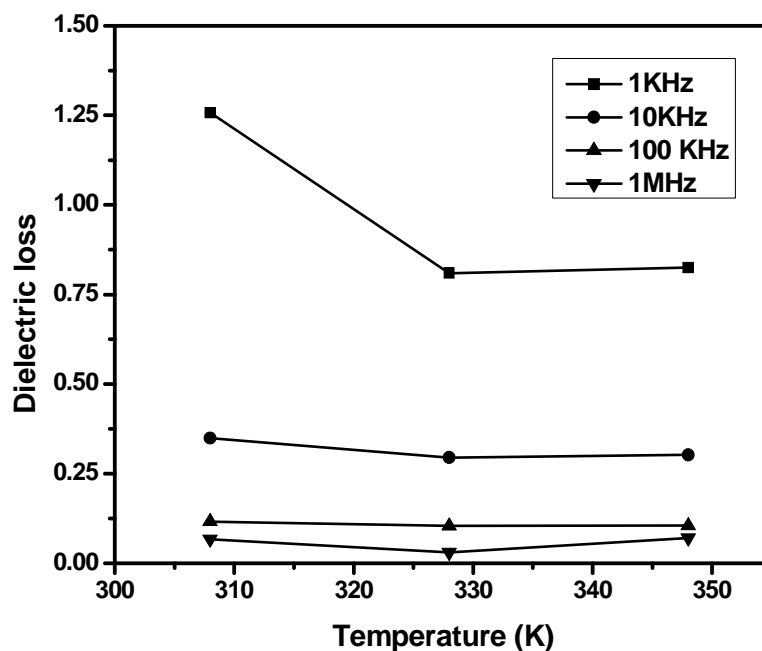


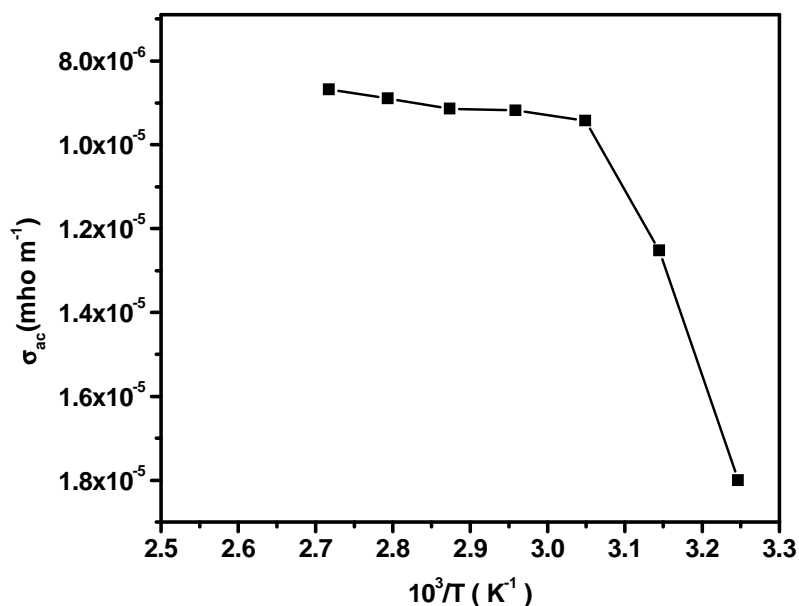
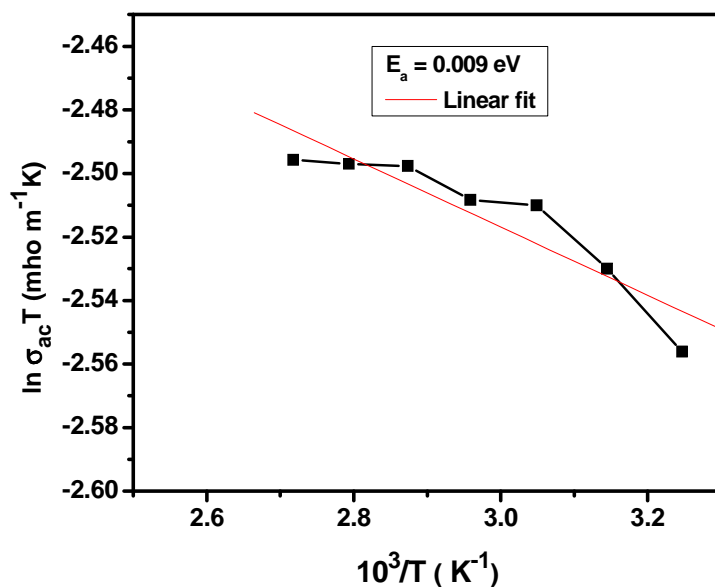
Fig. 12 Temperature dependence of dielectric loss for GGLY

3.4.2 *ac* conductivity study

The *ac* conductivity measurements are taken using HIOKI 3532-50 LCR HITESTER in the frequency range 50 Hz to 5 MHz. The sample is subjected to a temperature variation from 313 to 423 K. Temperature dependence of conductivity is shown in Fig. 13. The Arrhenius plot of σT versus $1000/T$ is shown in Fig. 14. It is evident from the graph that the conductivity increases with the temperature. Accordingly the value of activation energy for ionic migration is estimated from the slope of the Arrhenius plot. The line of best fit for the plot of $\log \sigma T$ versus $1/T$ obeys Arrhenius relationship.

$$\sigma = \sigma_0 \exp (E_a/kT)$$

Where σ_0 is the pre-exponent factor, E_a the activation energy for the conduction process and k is the Boltzmann constant. Therefore, the sample exhibits Arrhenius type conductivity behavior in the frequency range of investigation. The activation energy of GGLY for the conduction process, calculated from the plot is found to be 0.009 eV.

Fig. 13 Variation of *ac* conductivity with 1000/*T* for GGLYFig. 14 Plot of $\ln(\sigma_{ac})T$ versus 1000/*T* for GGLY

3.4.3 *dc* conductivity studies

The *dc* electrical conductivity (σ_{dc}) as a function of temperature is shown in Fig. 15. It is observed that conductivity increases with temperature indicating the temperature dependence activation energy (E_a) which is a characteristic of small polaron hopping (SPH) conduction mechanism. The plot of $\ln \sigma T$ versus 1000/*T* is shown in Fig. 16. The logarithmic conductivity in

the temperature range (313–423 K) exhibits almost linear dependence on reciprocal temperature ie. thermally activated behavior.

The SPH model is based on a strong coupling of electron with the lattice by a single phonon. According to this model the *dc* conductivity is given by

$$\sigma = \sigma_0 \exp(-E_d/kT)$$

Where σ_0 is a pre exponential factor, E_d is the activation energy, k is Boltzmann constant and T is temperature in K. The activation energy calculated from the slope of the graph (Fig. 16) it is found to be 0.045 eV. The low value of activation energy and high value of electrical conductivity are similar to those of LAO, LAM and MAN [20-22]. This result is in consistent with small polaron hopping theory [23].

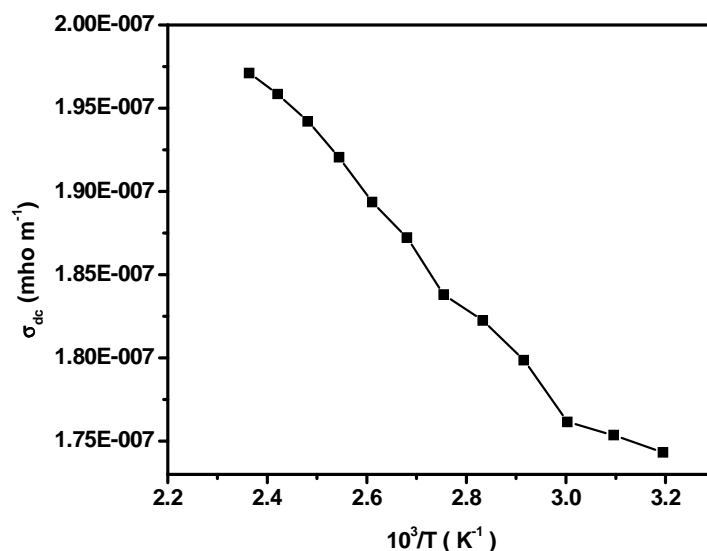


Fig. 15 Variation of *dc* conductivity with $1000/T$ for GGLY

3.5 Photoconductivity studies

Fig. 17 shows the plot of dark current and photo current against electric field. It is observed from the graph that both dark and photo currents increase linearly with the applied electric field, but the photo current is less than the dark current which is termed as negative photoconductivity. The negative photoconductivity in a solid is due to the reduction in the number of charge carriers or their life time in the presence of radiation [24]. The decrease in mobile charge carriers during negative photoconductivity can be explained by the Stockmann model [25].

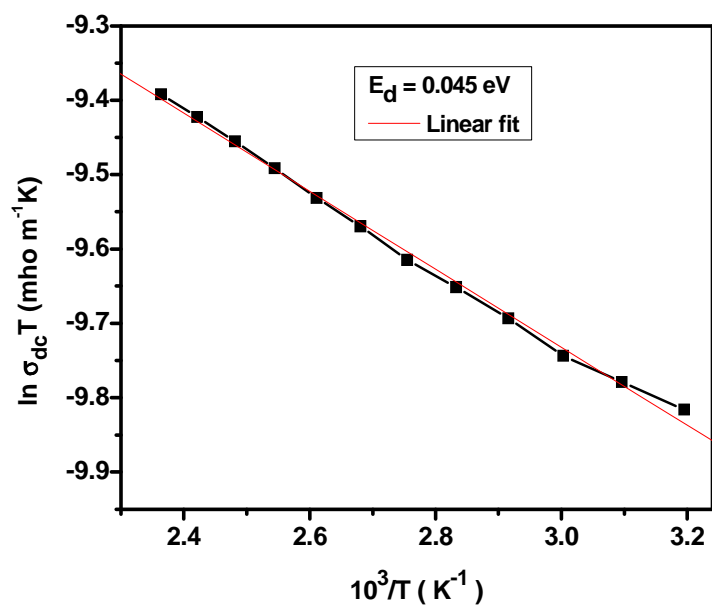
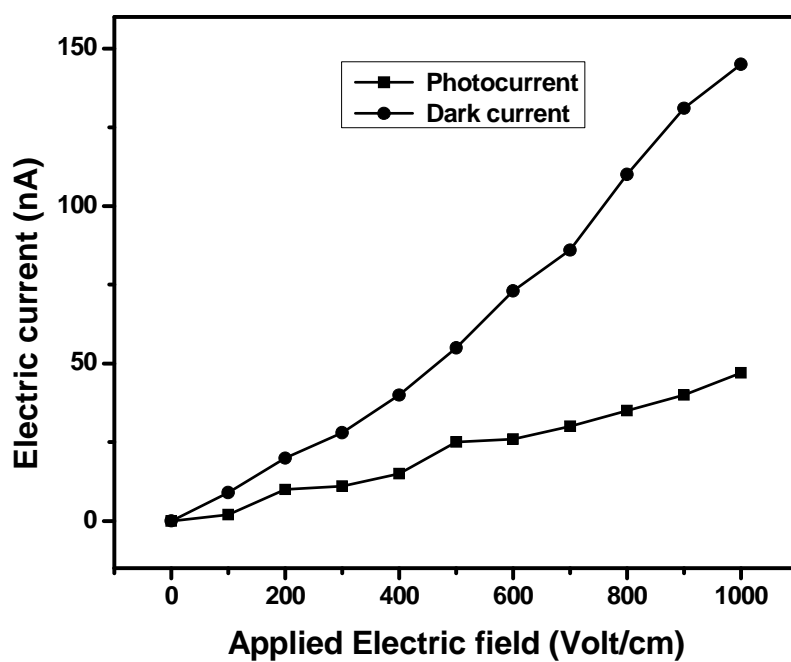
Fig. 16 Plot of $\ln(\sigma_{dc})T$ versus $1000/T$ for GGLY

Fig. 17 Field dependent photoconductivity of GGLY

CONCLUSION

The title compound of GGLY was successfully synthesized and the single crystals have been grown by solution growth technique. Its cell parameters have been determined by the single crystal XRD and powder XRD analysis. The presence of functional groups in gamma glycine has been identified from the FTIR analysis. Optical absorption study reveals the absorption edge at 350 nm. The phase matching natures of the grown crystals have been confirmed by Kurtz and Perry powder method. The microhardness measurements prove that gamma glycine belongs to the soft category of materials. The activation energy is determined from the plots of *ac/dc* conductivity. The negative photoconducting nature of the sample is confirmed by photoconductivity study.

Acknowledgement

The authors thank Dr. Babu Varghese, SAIF, IIT-Madras for their help and support.

REFERENCES

- [1] Prasad PN, Williams DJ, Introduction to Nonlinear Optical Effects in Molecules and Polymers, *Wiley-InterScience*, New York, **1991**.
- [2] Narayana Moolya B, Jayarama A, Sureshkumar M.R, Dharmaprakash S.M, *J. Cryst. Growth*, **2005**, 280, 581.
- [3] Albert L. Lehninger, Principles of Biochemistry, *CBS Publishers*, New Delhi, 1984.
- [4] Marsh RE, *Acta Crystallogr.*, **1958**, 11, 654.
- [5] Iitaka Y, *Acta. Crystallogr.*, **1960**, 13, 35.
- [6] Iitaka Y, *Acta. Crystallogr.*, **1961**, 14, 1.
- [7] Kunihiisa KS, *J. Crystal Growth*, **1974**, 23, 351.
- [8] Akihiko Ito, Maiko Yamanobe-Hada, Hitoshi Shindo, *J. Crystal Growth*, **2005**, 275, 1691.
- [9] Narayan Bhat MK, Dharmaprakash SM, *J. Crystal Growth*, **2002**, 236, 376.
- [10] Narayan Bhat MK, Dharmaprakash SM, *J. Crystal Growth*, **2002**, 242, 245.
- [11] Moolaya BN, Jayarama A, Sureshkumar MR, Dharmaprakash SM, *J. Crystal Growth*, **2005**, 280, 581.
- [12] Jan Baran, Henryk Ratajczak, *Spectrochimica Acta Part A*, **2005** 61, 1611.
- [13] Srinivasan K, Arumugham J, *Optic.Materials*, **2007**, 30, 40.
- [14] Ambujam. K, Selvakumar S, Prem Anand D, Mohamed G, Sagayaraj P, *Cryst. Res. Technol.*, **2006**, 41, 671.
- [15] Ramachandran E, Baskaran K, Natarajan S, *Cryst. Res. Technol.*, **2007**, 42, 73.
- [16] Kurtz SK, Perry T.T, *J. Appl. Phys.*, **1968**, 39, 3798–3813.
- [17] Onitsch E.M., ‘The present status of testing the hardness of materials’, *Mikroskopie*, **1956**, 95, 12-14.
- [18] Smyth CP, (1965) Dielectric behavior and structure, McGraw Hill, Newyork.
- [19] Balarew CP, Duhlew R, *J. Solid State Chem.*, **1984**, 55, 1-10.
- [20] Vimalan M, Ramanand A, Sagayaraj P, *Crys. Res. Technol.*, **2007**, 42, 1091- 1096.
- [21] Vimalan M, Cyrac Peter A, Rajesh Kumar T, Jayasekaran R, Packiam Julius J, Sagayaraj P, *Arch. Phy. Res.*, **2010**, 1 (2): 94-102.
- [22] Vimalan M, Helan Flora X, Tamilselvan S, Jeyasekaran R, Sagayaraj P, Mahadevan C.K, *Arch. Phy. Res.*, **2010**, 1 (3):44-53.

- [23] Mott BW, (1956) Microindentation Hardness testing, Butterworths, London.
- [24] Bube RH, (1981), Photoconductivity of Solids, Wiley Interscience, New York.
- [25] Joshi VN, (1990), 'Photoconductivity', Marcel Dekker, New York.